UDK 621.771.28:621.89
Original scientific article/Izvirni znanstveni članek

ISSN 1580-2949
MTAEC9, 42(2)59(2008)

LUBRICATION FLOW DURING THE ROLLING OF SEAMLESS TUBES

TOK MAZIVA PRI VALJANJU BREZŠIVNIH CEVI

Dušan Ćurčija[1], Ilija Mamuzić[2]

[1]Kneza Branimira 7, 44103 Sisak, Croatia
[2]Metallurgical faculty, University of Zagreb, Aleja narodnih heroja 3, 44103 Sisak, Croatia

Prejem rokopisa – received: 2007-10-12; sprejem za objavo – accepted for publication: 2008-01-10

An approximate analytical solution for calculating the lubricant-layer thickness for the continuous rolling of seamless tubes on a long, floating mandrel was derived. In the area of nano-behavior, the geometry of the process prevails over the rheological and kinematic characteristics. The solutions were derived for tools and tubes with smooth surfaces and offer the possibility of optimizing the quality of the lubricant. In calculations of the nano-lubricant layer, the thickness is assumed to be an artificial irrational value for maintaining the continuity of the mathematical analysis. This analysis justifies the use of new geometrical characteristics for the mandrel.

Key words: seamless tubes, rolling, lubrication

Razvita je bila približna analitska rešitev za izračun debeline maziva pri neprekinjenm valjanju brezšivnih cevi na plavajočem trnu. V območju nano obnašanja geometrija procesa prevlada nad reološkimi in kinematičnimi karakteristikami. Rešitev je razvite za orodja in cevi z gladko površinoin daje možnost za optimizacijo kakovosti maziva. Pri izračunu z nano debelino maziva, je debelina upoštevana kot umetna in irracionalna količina zaradi vzdrževanja kontinuitete matematične analize. Ta analiza opravičuje uporabo plavajočega trna z novo geometrijo.

Ključne besede: brezšivne cevi, valjanje, mazanje

1 INTRODUCTION

The rolling of tubes[1] in round passes is a variant of longitudinal rolling where, as a rule, and according to **Figure 1**, the two rolls and the mandrel form the zone of deformation[2]. The rolling with a long, floating mandrel occurs on a continuous rolling mill with seven to nine cages. Before the tube blank enters the rolling gap, a long, cylindrical mandrel is put into it, and then the mandrel moves in concordance with the rolled tube remaining in the zone of deformation. The mandrel's motion is slower than that of the tube front, but it is greater than the rate of the tube blank entering the gap between the rolls. The rolling speed is adjusted to obtain an equal speed of the tube and the rolls for every pass for a determined point of the cross-section of the deformation zone. In this way the curve of equal speeds of the tube and the rolls defines the range of relative sliding of metal, i.e., the zone of overtaking and the zone in arrears. It was proved experimentally[1] that during the rolling of the tube in several passes the overtaking takes place at the entrance of the tube in the gap between the rolls and the arrears at the exit of the gap between the rolls.

In recent years continuous rolling processes using long, fixed, cylindrical, conic or staged mandrels were developed. The rolling consists of two deformation zones: a zone for reduction of the tube's diameter, and a zone for the reduction of the tube's wall, as shown in **Figure 2**. No lubricant is added to the outside surface of the tube in contact with the rolls, and the friction[3] follows the Kulon-Amonton[4] law, while between the mandrel and the inside surface of the tube the friction occurs according to Newton's law. The tangential stress τ_x in the lubricant layer on the surface of the mandrel is described[5] by the differential equation:

$$\tau_x = \mu \cdot (v_C - v_T) \frac{1}{\varepsilon(x)} - \frac{1}{2} \varepsilon(x) \cdot \frac{\partial p}{\partial x} \qquad (1)$$

where μ is he dynamic viscosity of the lubricant, v_C and v_T are the speeds of the tube and the mandrel, $\varepsilon(x)$ is the

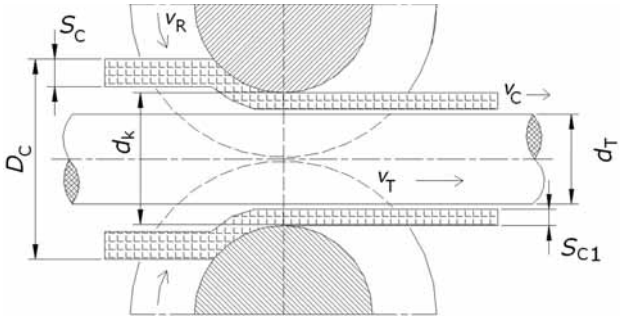

Figure 1: Scheme of rolling for seamless tubes on a long, floating mandrel: v_R – rolls peripheral velocity, v_T – mandrel motion velocity, v_C – tube motion velocity: S_C and S_{CI} – tube wall thickness before and after deformation, D_C; d_K, d_T, entrance and exit diameter of the tube and the diameter of mandrel

Slika 1: Shema valjanja brezšivnih cevi na dolgem plavajočem trnu: v_R – obodna hitrost valjev, v_T – hitrost premika trna, v_G – hitrost premika cevi, S_C in S_{C1} – vhodni in izhodni premer cevi in premer trna, D_C; d_K, d_T, vhodni in izhodni premer cevi in premer trna

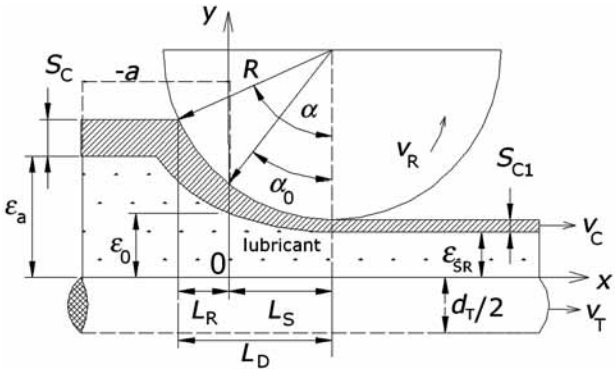

Figure 2: Two deformation sub zones in pass cross-section: L_R and L_S – zones of diameter and of wall reduction, ε_{SR} – average lubricant height on the mandrel in the last cage, α – engagement for tube blank pass angle, α_0 – angle of engagement deformation of the tube wall

Slika 2: Dve deformacijski podzoni na preseku prehoda: L_R in L_s – zoni redukcije premera in debeline stene, ε_{SR} – povprečna debelina maziva na trnu v zadnjem ogrodju, α – kot oprijema valjev na valjanec, α_0 – kot oprijema za deformacijo stene cevi

functional bond of the lubricant layer in Descartes coordinates, and $\partial p/\partial x$ is the partial gradient of the pressure in the lubricant layer along the x axis.

According[6] to **Figure 2**, for the lubricant consumption in the final cage of a continuous rolling mill, it is assumed that[7]:

$$\lim_{\varepsilon_a \to \varepsilon_0} (\alpha \to \alpha_0) \tag{2}$$

where ε_o is the lubricant-layer thickness at the entrance cross-section of the wall reduction for the angle α_o, and ε_a is the lubricant-layer thickness on the floating mandrel in the zone of reduction of the wall of the tube.

2 MATHEMATICAL DESCRIPTION OF THE LUBRICATION

According to **Figure 2** the process of lubrication of the mandrel and of the inside surface of the tube is described by the following Osborn-Reynolds differential equation[8].

$$\frac{\mathrm{d}p}{\mathrm{d}x} = \frac{6\mu(v_C + v_T)}{\varepsilon^2(x)} - \frac{12\mu Q}{\varepsilon^3(x)} \tag{3}$$

The specific consumption of lubricant per mandrel perimeter length is:

$$Q(x) = \int_0^{\varepsilon(x)} u\mathrm{d}y = -\frac{1}{12\mu}\frac{\mathrm{d}p}{\mathrm{d}x}\varepsilon^3(x) + \left(\frac{(v_C + v_T)}{2}\right)\varepsilon(x) \tag{4}$$

where u is the average speed of the lubrication motion, and dp/dx is the change of pressure in the lubricant layer alongside the x axis.

The following relation determines the thickness of the lubricant layer:

$$\varepsilon(x) = \varepsilon_0 + R_0\left[\cos\alpha_0 - \sqrt{1-\left(\sin\alpha_0 - \frac{x}{R_0}\right)^2}\right] \tag{5}$$

where $R_0 = R + S_{C1}$, R is the radius of the pass, and S_{C1} is the thickness of the tube wall in the last cage. The length of the lubricant wedge is calculated from:

$$a = R_0\left[\sqrt{1-\left(\cos\alpha_0 - \frac{\varepsilon_a}{R_0} + \frac{\varepsilon_0}{R_0}\right)^2} - \sin\alpha_0\right] \tag{6}$$

For the dressing processes the expression (5) can be developed to a power series:

$$\varepsilon(x) = \varepsilon_0 - \alpha_0 x + \frac{x^2}{2R_0} - \frac{\alpha_0 x^3}{2R_0^2} + \frac{x^4}{8R_0^3} \tag{7}$$

In this paper the shape of the lubricant layer on the mandrel in the area of (–a; 0) will be treated analytically. It is of interest for practical applications, for deducing the optimal lubricant layer thickness and for savings of high-quality lubricant.

3 CALCULATION AND DISCUSSION

By inserting the tube blank into a round pass gap the engagement occurs in the gap outlet, and after that the whole pass is gradually filled. The deformation process and, first, the shape of the section of the tube is changed from round to oval. During the following pass, the oval blank is turned by 90° and the longer axis of the rolled tube section is engaged in the rolling gap. The rolling is then continued in this sequence to the final pass. In the first cages of the continuous rolling mill the lubrication is in surplus in front of the inlet cross-section of the zone of deformation, while in the last cage the lubrication is insufficient in front of the inlet cross-section of the zone of deformation, and the lubricant layer is worn off. The lubricant behavior is explained from considering the **Figures 3 and 4**.

For the conditions of von Mizes plasticity:

$$k = \sigma_T/\sqrt{3} \tag{8}$$

where σ_T is the metal's deformation resistance and k is the constant of plasticity. The calculation will be developed on the basis of the pressure in the lubricant layer p_0 and the gripping angle of α.

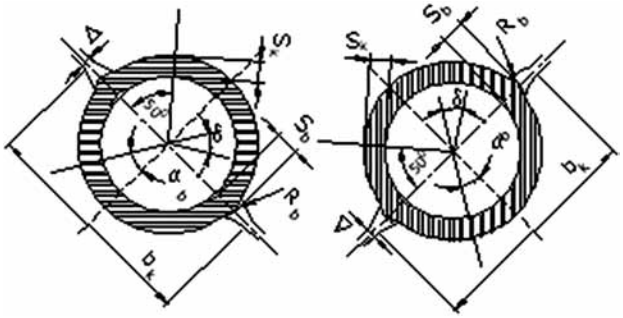

Slika 3: Okrogel prehod z zaokroženimi izhodi obrnjenimi za 90° v prvih dveh ogrodjih kontinuirne valjarne

Figure 3: Round pass with rounded outlets turned by 90° in the first two cages of the continuous rolling mill

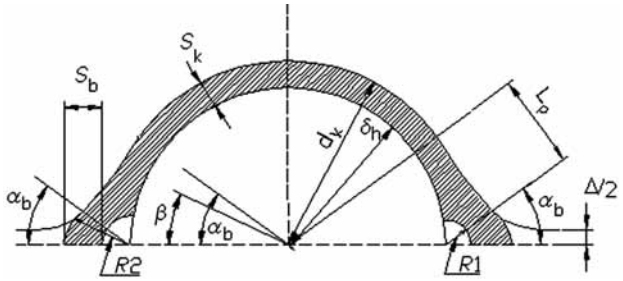

Figure 4: Detail of the round pass on the ninth cage of the continuous rolling mill $R1 \rightarrow R2 \rightarrow 0$. The wearing out of the lubricant is the most efficient at this rolling point.

Slika 4: Detail prehoda v devetem ogrodju kontinuirne valjarne $R1 \rightarrow R2 \rightarrow 0$. V tej točki valjanja je največja obraba maziva.

In **Table 1** the standard properties[9] of industrial lubricants according to the Russian standard C-24 (and data used for the following calculation) are given.

Table 1: The rheological, kinematic and geometric properties of lubricants[4,5]

Tabela 1: Reološke, kinematične in geometrične karakteristike maziv[4,5]

Parameter	Value	Unit
γ, pieso coefficient of viscosity	2.18E-7	Pa^{-1}
p_0, rolls pressure	20E6	Pa
v_C, motion speed of tube blank	8.5	m/s
v_T, mandrel speed	7.5	m/s
R, roll radius	0.197	m
S_{C1}	0.003	m
μ_0, dynamic viscosity of lubricant	0.024	Pa 8
α_0, engagement gripping angle	0-0.02	rad
ε_a, height of lubricant on the mandrel	0.001–0.0000001	m
A, technological parameter	1.965512E6	m^{-1}
$A = (1 - \exp(-\gamma \cdot p_0)/6\mu_0\gamma(v_C+v_T))$		
Smooth surfaces are assumed for the tube blanks and the mandrel $R_0 = R + S_{C1}$.		

The Barus dependence of lubricant viscosity on pressure is used, assuming a smooth surface for the mandrel and the tube:

$$\mu = \mu_0 \exp(\gamma \cdot p_0) \quad (9)$$

The results of the calculation of lubricant-layer thickness ε_0 at the gripping point in dependence of the gripping angle α_0 for the last cage of the continuous mill for $\varepsilon_a > \varepsilon_0$ is shown in **Figure 5**. By increasing the dynamic viscosity of the lubricant, ε_0 is also increased. The change of thickness ε_0 for the final cages of the continuous rolling line is linear.

The dependence of ε_a on ε_0^1 for the wearing out of the lubricant in the last cage of the continuous rolling mill stand is given in **Figure 6**. Series 1 presents the case when $\varepsilon_a >> \varepsilon_0$, and Series 3 and 5 for the cases when ε_a is in the micro- and nano-ranges, respectively. With the

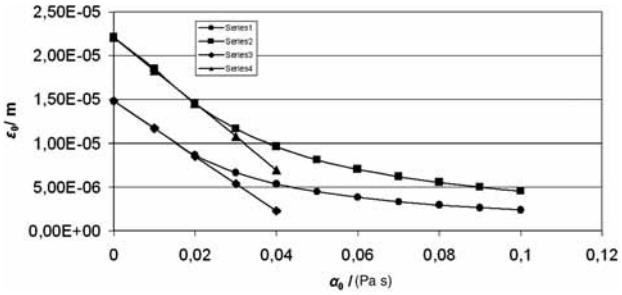

Figure 5: Influence of lubricant dynamical viscosity and the angle of engagement on the lubricant-layer thickness on the inlet cross-section of the wall-reduction zone

Series 1 – $\mu_0 = 0.024$ Pa s; Series 2 – $\mu_0 = 0.048$ Pa s; Series 3 and 4 – linearity through points $(0;\varepsilon_0^1)$ and $(\alpha_0^*; \varepsilon_0^*)$

Slika 5: Vpliv dinamične viskoznosti maziva in kota oprijema na debelino maziva na vhodnem preseku redukcije debeline stene cevi

Serija 1 – $\mu_0 = 0.024$ Pa s; Serija 2 – $\mu_0 = 0.048$ Pa s; Serije 3 in 4 – linearnost skozi točki $(0;\varepsilon_0^1)$ in $(\alpha_0^*; \varepsilon_0^*)$

entry in the nano-range, for example, for an extremely high intensity of lubrication wearing out, ε_0^1 practically does not undergo any changes when the dynamic viscosity of the lubricant increases. Then, the average thickness of the lubricant film ε_0 can determined if the final thickness of ε_0^1 is known.

In **Figure 7** the effect of $\Delta\varepsilon_0$ in the function ε_a^(1/3) is shown. The C belongs to Series 2, and its maximum is less well expressed. In the graphical representation, four zones are distinguished:

- the φ-zone of the first operative cages of the continuous stand, characterized by $\varepsilon_a >> \varepsilon_0$;
- the Ω-zone of the *mili* area of the lubricant layer ε_a, characteristic for the right-hand side of the continuous stand with relation to the point M;
- the ϕ-zone of the center of the continuous stand in the environment, and after the point M when for the lubricant layer the thickness is on the boundary of hydrodynamic lubrication;
- the Σ-nano-zone characterized by intensive wearing of the lubricant on the rolls of the last cage.

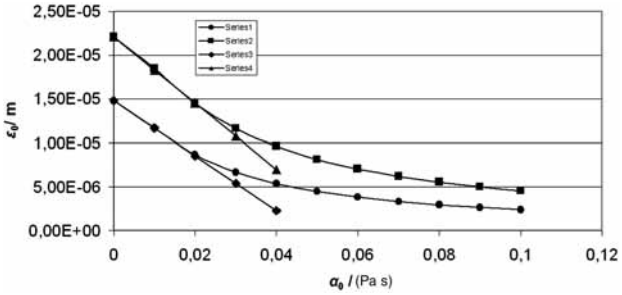

Figure 6: Effect of ε_a on ε_0^1 when $\alpha_0 \rightarrow 0$

Slika 6: Vpliv ε_a na ε_0^1 za $\alpha_0 \rightarrow 0$

Series/Serija 1 – $\varepsilon_a = 0.000\,942$ m;
Series/Serija 2 – $\varepsilon_a = 0.0000\,3141$ m;
Series/Serija 2 – $\varepsilon_a = 0.000\,000\,942$ m;
Series/Serija 4 – $\varepsilon_a = 0.000\,003141$ m;
Series/Serija 3 – $\varepsilon_a = 0.000\,000\,094205$ m

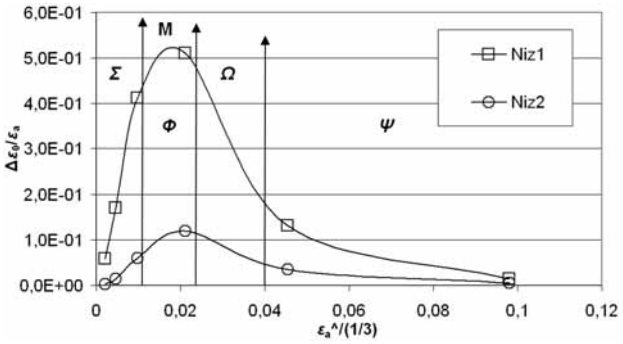

Figure 7: ε_a influence on deltas ε_0
Series 1, $(\varepsilon_0^1 - \varepsilon_0^{0.1}) / \varepsilon_a; \varepsilon_0^{0.1}$ – lubricant height for the angle of engagement of 0.1 rad; Series 2, $(\varepsilon_0^1 - \varepsilon_0^*) / \varepsilon_a$

Slika 7: Vpliv ε_a na delta ε_0
Serija 1, $(\varepsilon_0^1 - \varepsilon_0^{0.1}) / \varepsilon_a; \varepsilon_0^{0.1}$ – debelina maziva za orpijemni kot 0.1 rad; serija 2, $(\varepsilon_0^1 - \varepsilon_0^*) / \varepsilon_a$

The solutions of the differential Equation (3) in **Figures 5, 6, and 7** were obtained by applying the Monte-Carlo numerical method. We also tried to obtain approximate analytical solutions using the square polynomial in Equation (7). **Table 2** clearly shows this according to the marked areas in **Figure 7**.

Table 2: Approximate analytical solutions of the differential Equation (3) for the area of linearity.
Tabela 2: Aproksimativne analitične rešitve diferencialne enačbe (3) za področje linearnosti

Zone of Figure 7	Approximate analytical solution
Ψ	$\varepsilon_0^* = 0.7726\varepsilon_0^1 \quad \varepsilon_0^* = 0.5R_0(\alpha^*)^2 \quad \alpha^* = \sqrt[3]{\frac{8}{15R_0A}}$
Ω	$\alpha^* = 2 \cdot \sqrt[3]{\frac{\varepsilon_a\sqrt{2R_0\varepsilon_a}}{10R_0^2 + 15R_0A\varepsilon_a\sqrt{2R_0\varepsilon_a}}} \quad \varepsilon_0^* = \frac{R_0(\alpha^*)^2}{2}$
M	$\alpha_0^* = \left(\frac{2}{5}\right)^2 \frac{1}{A\varepsilon_{aMAX}} \quad \varepsilon_0^* = \frac{R_0(\alpha_0^*)^2}{2} \quad \varepsilon_{aMAX} = 0.28674 \cdot \sqrt[3]{\frac{R_0}{A^2}}$
Φ Σ	$\varepsilon_0^1 = \varepsilon_a\left(1 - \frac{0.57348\varepsilon_a}{\varepsilon_{aMAX}}\right) \quad \varepsilon_{aMAX} = 0.28674 \cdot \sqrt[3]{\frac{R_0}{A^2}}$
Note: indices (0 and *) refer to the discriminant of the trinomial of the second power in Equation (7) that limits to zero. The indices (0 and 1) are given for the case of $\alpha_0 \to 0$ rad. ε_{aMAX} = height of the lubricant layer on the mandrel at the maximum in **Figure 7**.	

The solution for the point M in **Table 2** can be used for the verification of numerical methods. The relations in the zone Ψ enable the linearity of the calculation presented in **Figure 5** and Series 3 and 4.

The comparison between the Monte-Carlo numerical method and the approximate analytical solutions in **Table 2** is given in **Table 3**. An acceptable matching of the results of both kinds of calculations is obtained. In a continuous rolling mill the stands before the inlet cross-section of the tube blank wall reduce the lubricant quantity, up to the point M, in a surplus over the quantity

Table 3: Comparison of Monte Carlo numerical method and analytical solutions in **Table 2** for the calculation of ε_0^*
Tabela 3: Primerjava numerične metode Monte Carlo in analitskih rešitev v **tabeli 2** za izračun ε_0^*

ε_a/m	Monte-Carlo ε_0^*/m	Zone Ω ε_0^*/m	Point M ε_0^*/m	Zone Φ, Σ ε_0^1/m
9.420E-04	1.225E-05	1.225E-05	-	-
8.735E-05	1.136E-05	1.129E-05	-	-
1.069E-05	5.801E-06	-	5.801E-06	-
7.425E-06	4.618E-06	-	-	4.466E-06
6.849E-06	4.373E-06	-	-	4.332E-06
1.210E-06	1.065E-06	-	-	1.081E-06
2.456E-07	2.362E-07	-	-	2.404E-07
1.205E-07	1.178E-07	-	-	1.192E-07
3.846E-08	3.809E-08	-	-	3.833E-08
1.046E-08	1.042E-08	-	-	1.045E-08
7.986E-09	7.962E-09	-	-	7.981E-09
4.123E-09	4.115E-09	-	-	4.121E-09
9.682E-09	9.676E-09	-	-	9.676E-09
3.141801E-10	3.1409E-10	-	-	3.1417E-10

that can be driven by the rolls into this zone. After ε_a entering the micro-area the opposite occurs, and wearing out of the lubrication takes place in the final stands of the continuous rolling mill. A similar effect is met during strip dressing, with the difference that the lubricant can be added before the rolls.

Table 3 presents filtered calculations according to the approximate analytical solutions in **Table 2**, obtained with a grapho-analytical approach. The domain of use for the zones Ω, Φ and Σ is determined by the common cross. It is necessary to point out that the Monte-Carlo numerical solution could also lead to conjugated-complex solutions for ε_0, and in the zones Φ and Σ. In this case it is necessary to increase Equation (7) with new members or start a new one with the original Equation (5). In areas where difficulties are found with the application of the numerical method, approximate analytical solutions are reliable. The solution for the lubricant abrasion on the mandrel in the last cages of the continuous rolling mill can be mastered with a proper geometrical relation of the mandrel and the working rolls. In new processes a graded mandrel is used to obtain more lubricant in the last cages of the rolling mill. A second geometrical solution for rolling with a mandrel with a constant section is based on the configuration of the rolls in the cages. A variant of this solution is shown in **Figures 3 and 4**.

4 CONCLUDING REMARKS

The effect of the lubricant-layer thickness ε_a on the lubricant-layer thickness on the rolling during the entering zone of the tube wall reduction ε_0 is analyzed for the longitudinal continuous rolling of seamless tubes using the long, floating mandrel. The calculation is made for the top of the rolling pass, which is in each subsequent cage turned by 90°. It can be considered that up

to point M in **Figure 7**, stable hydro-dynamical lubricating occurs. This means that the first and the second cages will be supplied with a surplus and the next cages with a shortage of lubricant. This shortage will be even greater in the last cages of finishing the tube with the final dimensions. In this position, the gripping angle for wall reduction approaches zero and ahead of the cage the quantity of lubricant is lower than that which could be driven in the deformation zone, and a shortage of lubricant is met. To overcome this problem the solution of Equation (2) was proposed in the graphical approach to a limit as the gripping angle approaches zero (by lowering the wall thickness Equation (2) approaches the mathematical definition for a limit). Equation (10) was developed for this case.

$$\varepsilon_0^1 = \varepsilon_a \left(1 - \frac{0.57348\varepsilon_a}{\varepsilon_{aMAX}} \right) \quad \varepsilon_{aMAX} = 0.28674 \cdot \sqrt[3]{\frac{R_0}{A^2}} \quad (10)$$

which is in acceptable agreement with the Monte-Carlo method.

The dependence in **Figure 7** allows us to make the following conclusions:

– with a small lubricant thickness on the mandrel (εa), in the zone of the wall deformation (ε_a); the effect of the process kinematics and of the lubricant rheology on the lubricant-layer thickness on the mandrel is greater than the effect of the rolling geometry;
– point M in **Table 2** makes it possible for us to calculate the lubricant-layer thickness at the initial state of the wall reduction, and this could be used to verify the transient Monte-Carlo solution for the same conditions;
– in the exit stands, when the lubricant-layer thickness on the mandrel (ε_a) approaches the boundary to the micro- and the nano-areas because the lubricant is worn out, the effect of the rolling geometry on the lubricant thickness in the deformation zone (ε_0) becomes stronger. The theoretical case of ε_a in the nano-area is analyzed and according to **Table 3** a good agreement was achieved with the Equations (10) and the numerical integration. This conclusion justifies the use of the graded mandrel in the rolling technology;
– for the theoretical analysis of the lubricant-layer thickness on the mandrel ahead of the zone of tube wall deformation, the solutions in **Table 2** are reduced to a triple point, which can be mathematically written according to relation (11).

$$\lim_{\substack{\varepsilon_a \to \varepsilon_0^1 \to \varepsilon_0^* \\ \alpha_0 \to 0}} [\text{equation (3)}] \to [\text{equation (10)}] \quad (11)$$

Thus, the solution of Equation (3) is the approach to the analytical relation (10). This is clear from **Figure 5**, where the increase in the dynamic viscosity cannot help to increase the lubricant-layer thickness in the zone of reduction of the wall thickness in the case when the lubricant-layer thickness on the mandrel (ε_a) decreases to the nano- range and the gripping angle for the tube approaches zero. Series 5 is calculated for the mandrel lubricant-layer thickness from 0 m to 0.000094205 m; it has a low angle to the abscissa (lubricant dynamical viscosity) and can be considered as constant for the average mandrel layer thickness and virtually independent of the zone of calculation in **Table 2**.

In this area the numerical Monte-Carlo method will give complex conjugated solutions. The approach has a synthetic irrational figure for the mandrel lubricant-layer thickness ahead of the point of the initial wall reduction on the basis of the irrational value of two ($\sqrt{2}$), which is included in ε_a.

5 REFERENCES

[1] I. Mamuzić, V. M. Drujan, Teorija, Materijali, Tehnologija, Čeličnih cijevi, Hrvatsko Metalurško Društvo, Zagreb 1996, 137–275

[2] S. V. Mazur, Postanovka zadači i zakonomernosti tečenija smazki v očage deformacii pri prokatke trub, Sučasni problemi metalurgii, 8 (**2005**), 447–452

[3] D. Ćurčija, I. Mamuzić, Mater. Tehnol., 39 (**2005**) 3, 61–77

[4] O. P. Maksimenko, A. A. Semenča, Issledovanie kontaktno-gidrodinamičeskoj smazki pri prokatke. Sučasni problemi metalurgii, 8 (**2005**), 99–103

[5] P. L. Klimenko, Kontaktniie naprjaženija pri prokatke s tehnologičeskoj smazkoj, Sučasni problemi metalurgii, 8 (**2005**), 44–49

[6] D. Ćurčija, Mater. Tehnol., 37 (**2003**) 5, 237–251

[7] D. Ćurčija, I. Mamuzić, Metalurgija 44 (**2005**) 3, 221–226

[8] D. Ćurčija, I. Mamuzić, Metalurgija 44 (**2005**) 4, 295–300

[9] D. Ćurčija, I. Mamuzić, Lubricating film shape at band dressing, 38 Symposium Lubricants, Društvo za Goriva i Maziva, Zagreb, Rovinj 19–21 10, 2005. Croatia (will by publisehed)